

ANALYTICAL STUDY ON QUALITY EVALUATION OF EMBANKMENT STRUCTURE WITH A VIEW TO LONGER LIFE

Emika Nakamura¹ and *Shin-ichi Kanazawa²

¹ Social Environmental Systems Engineering Course, National Institute of Technology, Fukushima College, Advanced Course Program, Japan

² Civil and Environmental Engineering, National Institute of Technology, Fukushima College, Japan

*Corresponding Author, Received: 15 June 2020, Revised: 30 Nov. 2020, Accepted: 17 Jan. 2021

ABSTRACT: In recent years, the demand for quality evaluation of earth structures has increased, coupled with the strong demand for cost reduction in construction projects. In order to respond to such social movements, it is urgent to carefully consider the design conditions and processes of the earth's structure. At present, the machinists and engineers at the site are improving, and it is necessary to consider the construction conditions that lead to the quality evaluation of the embankment over the long term. On the other hand, in the future, it will be necessary to simplify work such as high-speed construction and unmanned driving using AI. Therefore, in this study, stress changes in the long-term service process are evaluated by performing analysis while changing the embankment construction conditions and climatic conditions. As a result of these analyzes, it was confirmed that the climatic conditions are more likely to change the stress state of the embankment than the construction conditions. It will extend the life of the embankment and shorten the construction period.

Keywords: Embankment, Longer life, Cost reduction, Finite element method

1. INTRODUCTION

Soil structures are compacted to improve stability and deformation characteristics. However, many cases of dikes collapse due to local torrential rains and typhoon torrential rains have been reported, and the collapse mechanism has not been completely clarified. The stability of the embankment against heavy rainfall is considered to depend strongly on four factors: the treatment of the foundation ground, the quality of the embankment material, the degree of compaction, and the treatment of water [1]. Among these, the cause of embankment collapse in many cases is the treatment of water.

Although embankment structures are initially properly drained according to land and environmental conditions, embankments frequently collapse. One causal factor is that the construction and maintenance of the embankment depends on engineer experience.

Soil consists of three phases: a solid phase, liquid phase and gas phase, and the embankment and underlying ground below the water table are often in an unsaturated state containing air or dissolved air. It is considered that gas is dissolved and released into the liquid phase as the pore air pressure changes due to rainfall infiltration, resulting in volume compression. As a result, it is possible that current construction guidelines do not have sufficient drainage measures and embankment maintenance requirements to withstand recent heavy rainfall. In addition, drainage measures for the embankment and the time at which it is affected

by rainfall are important factors. It is thought that the influence of rainfall during construction weakens the inside of the embankment, but timing of construction cannot be fixed, and the amount of rainfall received during construction varies.

In addition, construction is generally not carried out in the rainy season, but in some cases this is unavoidable. To counter these adverse weather conditions, drainage measures are taken while paying attention to the weather, but the effects of rainfall during construction and the effect of the initial stress state at the completion of embankment have not been clarified. At normal sites, the embankment is exposed to climatic conditions, such as repeated dry and wet conditions, and the effects of the behavior of unsaturated soil cannot be ignored. Therefore, in order to obtain a precise initial stress state, it is necessary to consider the influence of the dry and wet mechanical conditions. It is also necessary to propose a method for estimating the initial stress state in consideration of the dry and wet mechanical conditions, such as rainfall and evaporation.

In addition, mechanical construction capability on site and the experience of engineers are improving, and it is necessary to study the construction conditions that will lead to high quality embankment from a long-term perspective. Additionally, in the future, simplification of work, such as high-speed construction using AI and unmanned operation will be required [2].

In this study, embankment analysis considering compaction and rainfall / evaporation history is

performed using soil / water / air coupled finite analysis code. Differences in compaction strength of the embankment, layer thickness of construction, and the amount of rainfall are analyzed, and stress change during the long-term service process are evaluated. This analysis contributes to shortening the construction period with a view to extending the life of the embankment. In addition, by grasping the mechanical behavior inside the embankment through this analysis, this study also aims to enable understanding the design needed for required performance of the embankment in the future.

2. RESEARCH METHOD

2.1 Soil/Water/Air Coupled Finite Analysis Code

The finite element analysis code (DACSAR-MP) [3] used in this study formulates the unsaturated soil constitutive model proposed by Ohno et al [4]. This model is framed as the soil/water/air coupled problem using the three-phase mixture theory. This study proposes a model in which the effective degree of saturation is used as the state quantity to represent rigidity, by referring to the model of Karube et al, which defines effective stress considering water content [5]. Equation (1) shows the effective stress. Equation (2) shows the base stress tensor and suction stress. Equation (3) shows suction.

$$\boldsymbol{\sigma}' = \boldsymbol{\sigma}^{\text{net}} + p_s \mathbf{1} \quad (1)$$

$$\boldsymbol{\sigma}^{\text{net}} = \boldsymbol{\sigma} - p_a \mathbf{1}, p_s = S_e s \quad (2)$$

$$s = p_a - p_w, S_e = \frac{S_r - S_{rc}}{1 - S_{rc}} \quad (3)$$

Here, $\boldsymbol{\sigma}'$ is the effective stress tensor; $\boldsymbol{\sigma}^{\text{net}}$ is the base stress tensor; $\mathbf{1}$ is the second order unit tensor; $\boldsymbol{\sigma}$ is the total stress tensor; s is the suction; p_s is the suction stress; p_a is the pore air pressure; p_w is the pore water pressure; S_r is the degree of saturation; S_e is the effective degree of saturation; and S_{rc} is the degree of saturation at $s \rightarrow \infty$. In numerical calculations, the EC model of Ohno et al. [6], which does not have a singularity in the yield surface, was incorporated to avoid shifting to the singularity, a quantity impossible to differentiate, during preconsolidation pressure at saturation. Equations (4), (5), (6) and (7) provide the yield function.

$$f(\boldsymbol{\sigma}', \zeta, \varepsilon_v^p) = MD \ln \frac{p'}{\zeta p_{sat}} + \frac{MD}{n_E} \left(\frac{q}{Mp'} \right)^{n_E} - \varepsilon_v^p = 0 \quad (4)$$

$$\zeta = \exp \left[(1 - S_e)^{n_s} \ln a \right], MD = \frac{\lambda - \kappa}{1 + e_0} \quad (5)$$

$$p' = \frac{1}{3} \boldsymbol{\sigma}' : \mathbf{1}, q = \sqrt{\frac{3}{2} \mathbf{s} : \mathbf{s}} \quad (6)$$

$$\mathbf{s} = \boldsymbol{\sigma}' - p' \mathbf{1} = \mathbf{A} : \boldsymbol{\sigma}', \mathbf{A} = \mathbf{I} - \frac{1}{3} \mathbf{1} \otimes \mathbf{1} \quad (7)$$

Here, n_E is the shape parameter; ε_v^p is the plastic volume strain; M is the q/p' in the limit state; D is the dilatancy coefficient; p_{sat} is the yield stress at saturation; a and n_s are the parameters representing the increase in yield stress due to unsaturation; λ is the compression index; and κ is the expansion index. Equation (8) shows pore water velocity. Equation (9) shows air velocity. Pore water and air flow follow Darcy's law.

$$\tilde{v}_w = -\mathbf{k}_w \cdot \text{grad} h \quad (8)$$

$$\tilde{v}_a = -\mathbf{k}_a \cdot \text{grad} h_a, h_a = \frac{p_a}{\gamma_w} \quad (9)$$

Here, \tilde{v}_w is the pore water velocity; \tilde{v}_a is the air velocity; \mathbf{k}_w is the hydraulic conductivity; \mathbf{k}_a is the coefficient of air permeability; h is the total head; γ_w is the unit weight of water; and h_a is the pneumatic head. Equations (10)-(11) show hydraulic conductivity and the coefficient of air permeability by way of Mualem's [7] formula and the Van Genuchten [8] formula.

$$\mathbf{k}_w = k_{rw} \mathbf{k}_{wsat} = S_e^{1/2} \left[1 - (1 - S_e^{1/m})^m \right]^2 \mathbf{k}_{wsat} \quad (10)$$

$$\mathbf{k}_a = k_{ra} \mathbf{k}_{ares} = (1 - S_e)^{1/2} (1 - S_e^{1/m})^{2m} \mathbf{k}_{ares} \quad (11)$$

Here, k_{rw} is the ratio of hydraulic conductivity; k_{ra} is the ratio of coefficient of air permeability; m is the Mualem constant; \mathbf{k}_{wsat} is the hydraulic conductivity at saturation; \mathbf{k}_{ares} is the coefficient of air permeability in dry conditions. Equations (12)-(13) show the continuous formula of pore water and air using three-phase mixture theory.

$$n \dot{S}_r - S_r \dot{\varepsilon}_v + \text{div} \tilde{v}_w = 0 \quad (12)$$

$$(1 - S_r) \dot{\varepsilon}_v + n \dot{S}_r - n(1 - S_r) \frac{\dot{p}_a}{p_a + p_0} - \text{div} \tilde{v}_a = 0 \quad (13)$$

Here, n is porosity; $\dot{\varepsilon}_v$ is volumetric strain; and

p_0 is atmospheric pressure. The elasto-plastic constitutive model obtained from Equation (4) and the equilibrium equation [Equations (12) - (13)] are formulated as the soil/water/air coupled problem.

3. STRESS ANALYSIS DURING THE SERVICE PROCESS

3.1 Analysis Condition

In this study, embankment analysis of embankment structure considering rainfall and evaporation was performed using unsaturated soil / water / air coupled finite element method analysis program (DACSAR-MP). Table 1 shows the material parameters used in the analysis, and Figure. 1 shows the moisture characteristic curve, where λ :the swelling index, κ : the compression index, $M = (p/q)$:the stress ratio, n_E : the fitting parameter of the EC model, a :parameter for determining the magnification of consolidation yield stress due to desaturation, m : unsaturated hydraulic conductivity parameters, S_{r0} : saturation of adsorbed water, k_a : air permeability coefficient, v : Poisson's ratio, G_s : soil particle specific gravity, and k_w : saturated hydraulic conductivity.

The analysis area is assumed to be foundation ground measuring 15m in length x 45m in width, with embankment 3m wide at the top, 15m wide at the bottom and 6m high. The foundation ground has a saturation level of 50% up to 3m from the ground surface, and a 90% saturation level deeper than 3m from the ground surface. The displacement boundary was fixed vertically and horizontally at the lower end of the foundation ground, and the hydraulic boundary was drained at the top and bottom and undrained at the left and right.

Table 1 Material parameters

λ	κ	M	m	S_{r0}	k_a (m/day)
0.18	0.037	1.33	0.8	0.15	1.0
n	n_E	a	v	G_s	k_w (m/day)
1.0	1.3	10.0	0.33	2.7	0.01

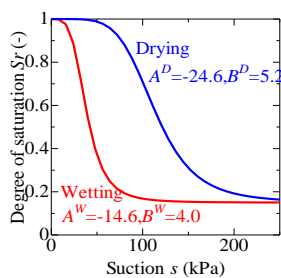


Fig.1 Soil water characteristic curve

3.1.1 Stress analysis conditions in the service process due to differences in construction conditions

In this study, layer thickness and compaction strength are considered as construction conditions.

Compaction was expressed by loading and unloading each layer under the load conditions of 300, 600, and 900kPa, after construction at 0.3 and 0.6m layer thicknesses during a construction period of one month. Figure.2 shows the analysis area at a layer thickness of 0.3m, and Figure.3 shows the analysis area at 0.6m.

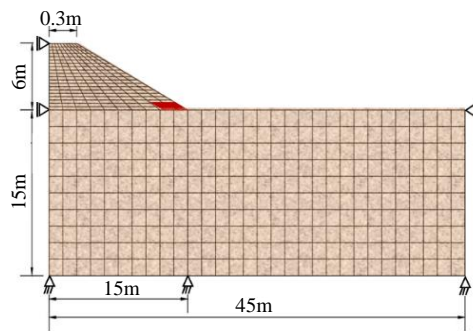


Fig.2 Analysis area with a thickness of 0.3m

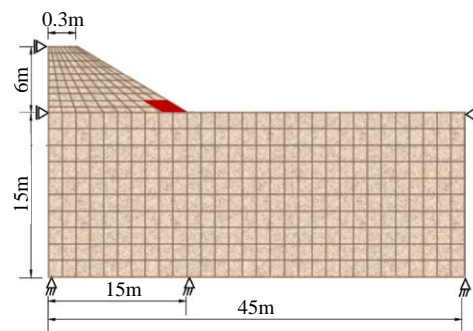


Fig.3 Analysis area with a thickness of 0.6m

3.1.2 Stress analysis conditions in the service process due to differences in climatic condition

In this study, rainfall during construction is considered a climatic condition. Because the amount of precipitation changes from month to month, the amount of precipitation the embankment receives during the civil engineering work will differ depending on month in which the construction is implemented. Therefore, by changing the construction time, the stress change due to differences in rainfall during construction will be investigated and compared. The rainfall history used in this study is shown in Figure.4. For the rainfall applied during construction, the annual rainfall history of Fukuoka City in Fukuoka Prefecture in 2010 was used to simulate average

rainfall in Japan. For stress analysis during embankment service due to the differences in construction conditions, total rainfall of 1729 mm was corrected to one month, and rainfall of 144.1 mm was applied. For stress analysis in service due to different climatic conditions, we prepared 3 cases with characteristic rainfall, as shown in Figure.4.

These three cases provide the lowest rainfall in January, the highest rainfall July, and an average rainfall in April; i.e. 50.5mm in January, 199.5mm in April, and 453.5mm in July. These rainfall conditions were applied throughout construction, and then the embankment analysis was performed.

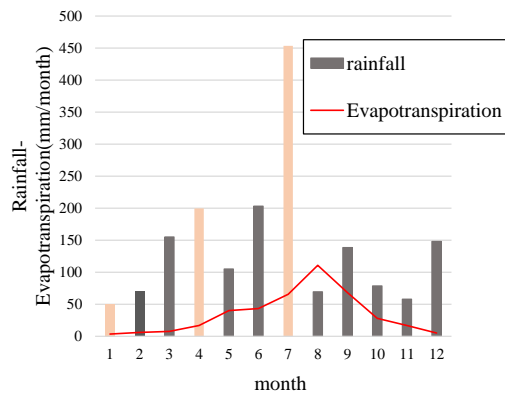


Fig.4 Fukuoka Prefecture monthly rainfall and evaporation history (2010) [9]

3.2 Analysis Result

3.2.1 Stress analysis results in the service process due to differences in construction conditions

Figure.5 to 8 show the initial stress distributions under load conditions of 300, 600, and 900kPa, divided into layer thicknesses of 0.3 and 0.6m, respectively.

From the average effective principal stress distribution in Figure.5, no significant difference due to the difference in rolling compaction strength (300, 600, 900kPa) can be confirmed. The same is true when looking at the comparison based on layer thickness (0.3m, 0.6m). One notable difference is that the layer boundary at the layer thickness of 0.6 m is clearer than the distribution of layer boundaries at the layer thickness of 0.3m.

In all stress distributions, the average effective principal stress in the foundation ground is large, and the void ratio distribution is small, as shown in Figure.7. This suggests that the embankment fully reflects the compaction effect from the e -log P' relationship. In the degree of saturation distribution shown in Figure.6, a discontinuity at the layer boundary of the embankment is apparent. From these visualizations, embankment with a layer thickness of 0.6m has a larger discontinuous surface than with a layer thickness of 0.3m, which tends to

affect the compaction performance. Thus, although a change in the stress distribution due to the difference in layer thickness could be confirmed, there was no significant difference due to the compressive strength.

Next, from the void ratio distribution in Figure.7, it can be seen that there is a tendency for expansion due to the large void ratio value in the surface layer of the embankment, which indicates loose compaction of this region. It also seems that there is a change in the surface layer of the embankment at layer thicknesses of 0.3m and 0.6m. However, as the difference in value is about 0.001, it can be said that there is no significant difference due to layer thickness. Also, no significant difference due to compressive strength can be confirmed.

Finally, from the shear strain distribution shown in Figure.8, it can be confirmed that the morphology of surface slip has already appeared; although, the fracture risk is low because of the low shear distribution value. Therefore, caution is advised in these cases, as the surface layer may be damaged if it is affected by heavy rain after construction.

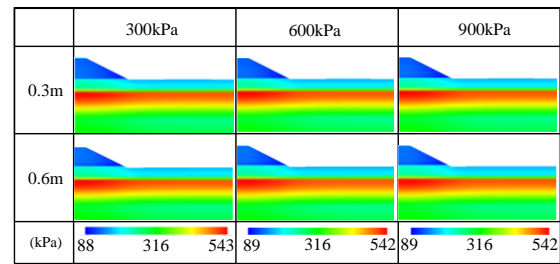


Fig.5 Effective mean stress p'

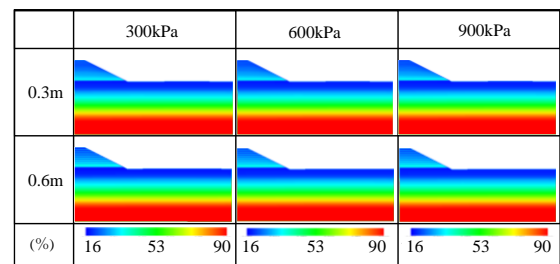


Fig.6 Degree of saturation S_r

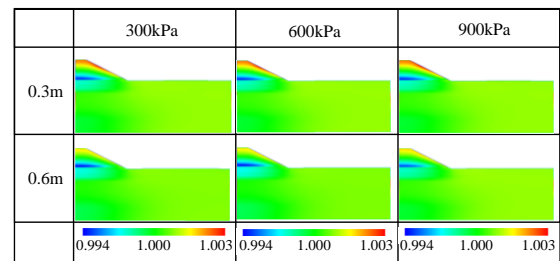


Fig.7 Void ratio e

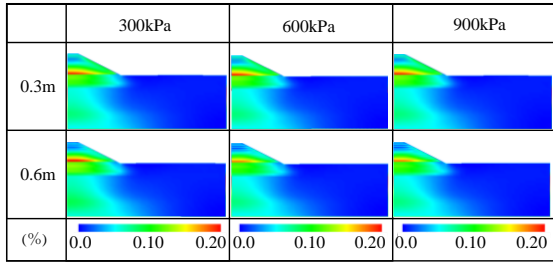


Fig.8 Shear Strain ϵ_s

From the above, it can be said that there was almost no change in the initial stress due to the difference in rolling strength (300, 600, 900kPa), and there was no significant change due to the layer thickness (each initial stress value) (0.3, 0.6m). However, at a layer thickness of 0.6m, large discontinuities occur at the layer boundaries, suggesting that different layer thicknesses affect compaction performance.

In summarizing the results of the initial stress analysis due to the difference in the construction conditions, it can be said that the differences in the layer thickness and load conditions, which are the construction conditions, have little effect on each initial stress.

3.2.2 Stress analysis results in the service process due to differences in climatic conditions

This section describes the results of embankment analysis at applied rainfall of 50.5mm in January, 199.5mm in April, and 453.5mm in July. However, when comparing the initial stress distributions with different rolling strengths for each construction time by layer thickness, no stress change due to different loading conditions could be confirmed at any construction time. In examining this, it was determined that carrying out the stress analysis only for the embankment with a compaction strength of 300kPa would yield valid results. Therefore, Figure 9 to 12 show the outline of each stress distribution of each layer thickness when the construction time was changed, using the analysis results at the compressive strength of 300kPa.

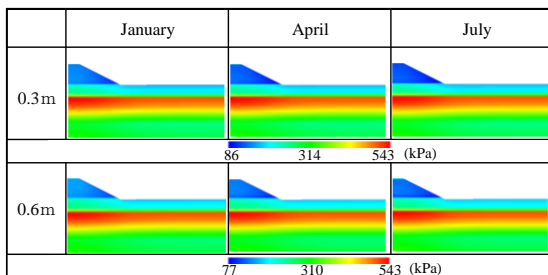


Fig.9 Effective mean stress p'

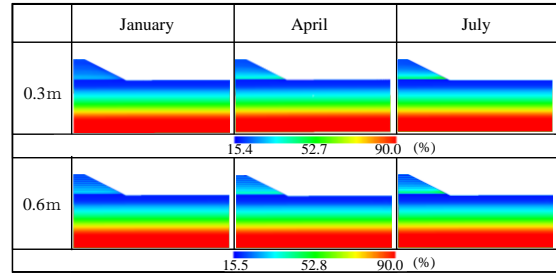


Fig.10 Degree of saturation S_r

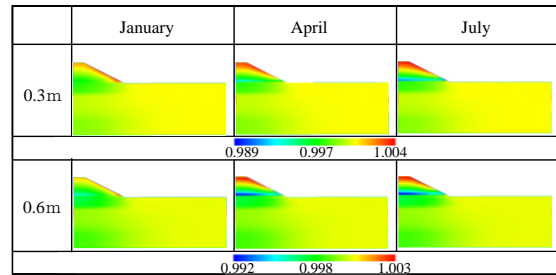


Fig.11 Void ratio e

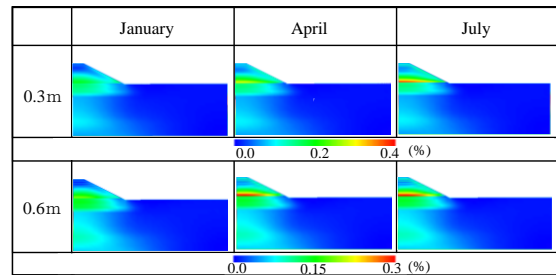


Fig.12 Shear Strain ϵ_s

From Figure.9, it can be confirmed that the effective stress in the embankment decreases as the amount of rainfall applied during construction increases. In addition, the distribution of the void ratio, as shown in Figure.11, increases at the embankment surface layer in the order of January, April, and July. From these tendencies, it can be said that the embankment surface layer is loosely compacted. Furthermore, the value of the void ratio in the lower part of the embankment becomes smaller as the amount of rainfall increases, which suggests that the self-weighting effect of rainfall causes the interior of the embankment to become dense. A similar tendency can be confirmed from the shear strain distribution in Figure.12. Also, although the shear strain in the surface layer of the embankment is large and the surface slip takes form, the risk of fracture is low at this point because the value is small. No significant difference in stress distribution due to layer thickness could be confirmed. As described above, changes in initial stress distribution due to differences in construction time, that is, differences due to rainfall during

construction, were confirmed. In other words, it was found that levees constructed during periods of low rainfall were stronger than levees constructed during periods of high rainfall. The higher the rainfall, the higher the risk of damaging the weaker embankment surface.

4. CONCLUSION AND FUTURE OUTLOOK

From the results of this study, it was possible to confirm the effects of differences on the stress inside the embankment in construction conditions, which depended on the compaction strength and the layer thickness of the embankment, as well as climatic conditions, which depended on season of construction. The stress analysis results during embankment service due to the difference in construction condition confirmed no change in the load conditions compared in this study but a difference in the size of the discontinuous surface that formed. As a result, there is almost no difference in compressive strength (300, 600, 900 kPa) and layer thickness (0.3m, 0.6m) due to differences in construction conditions over a long period of time. Therefore, at the present time, no problems are anticipated with carrying out the embankment construction a compressive strength of 300kPa, which can reduce costs, and a layer thickness of 0.6m, which can shorten the construction period.

The stress analysis results during embankment service due to the difference in climatic conditions confirmed that dikes constructed during the low rainfall season are stronger than dikes constructed during the high rainfall season. In other words, it is advisable to build levees during periods of low rainfall. However, it is necessary to continue studying heavy rainfall after construction and changes in stress distribution after several years.

In summary, climatic conditions are more likely to change embankment stress conditions than construction conditions. Disaster prevention management during continuous rainfall is also carried out mainly based on the observation results of rainfall, and is used as a collapse prediction method. Therefore, it can be said that climatic conditions are very important for embankment not only at the embankment stage but also after embankment [10]. Therefore, it can be said that climatic conditions are very important not only during construction but also in the embankment after completion. However, these results are only trends at this stage. In the future, we would like to study additional construction conditions and climatic conditions and consider various process scenarios. The changes in stresses during long-term

use of levees can also be assessed by analytically examining how these differences change the internal stresses of levees after decades. From the viewpoint of extending the life of these structures, it is also possible to conduct feedback analysis after the embankment is constructed and to monitor vulnerable points.

5. REFERENCES

- [1] Japan Road Association, Road earthwork-Embankment work guidelines, 2010.
- [2] Hujino K., Hashimoto T., Yuta S., Tateyama K., Study on effective method to select a suitable operator for unmanned construction system, Journal of JSCE, Vol.74, No.1, pp.11-17, 2018.
- [3] Kanazawa S., Tachibana S., Izuka A., Analytical study on drainage capacity of embankment structure, JSCE, Vol.71, pp.429-436, 2015.
- [4] Ohno S., Kawai K. and Tachibana S., Elastoplastic constitutive model for unsaturated soil applied effective degree of saturation as a parameter expressing stiffness, Journal of JSCE, Vol.63, No.4, pp.1132-1141, 2007.
- [5] Karube D., Kato S., Hamada K. and Honda M., The relationship between the mechanical behavior and the state of porewater in unsaturated soil, Journal of JSCE, No. 535, III34, pp.83-92, 1996.
- [6] Ohno S., Iizuka A. and Ohta H., Two categories of new constitutive derived from non-linear description of soil contractancy, Journal of JSCE, Vol.9, pp.407-414, 2006.
- [7] Mualem Y., A new model for predicting the hydraulic conductivity of unsaturated porous media, Water Re-sources Research, Vol.12, No.3, pp.514-522, 1976.
- [8] Van Genuchten, A closed-form equation for predicting hydraulic of unsaturated soils, Soil Science Society American Journal, Vol.44, pp.892-898, 1980.
- [9] Japan Meteorological Agency, Japan Meteorological Agency, <http://www.jma.go.jp/jma/index.html>.
- [10] Nishi K., Fukukawa K., Ogawa T. and Nakagawa K., A System for forecasting cut-off slope collapse during continuous heavy rain, Journal of JSCE, Vol.24, No.498, pp.95-104, 1994.

Copyright © Int. J. of GEOMATE. All rights reserved, including the making of copies unless permission is obtained from the copyright proprietors.
